MICRONEEDLE PATCH FOR ENHANCED TRANSDERMAL DELIVERY OF ANTIHISTAMINE – AN INNOVATIVE APPROACH

AWAIS MAQBOOL,[*] ZULCAIF,[**] ASIF MAHMOOD,[**] HIRA IJAZ[***] and RAI MUHAMMAD SARFRAZ[****]

[*]*Riphah Institute of Pharmaceutical Sciences (RIPS), Riphah International University, Lahore Campus, Lahore, Punjab, Pakistan*
[**]*Department of Pharmacy, University of Rasul, Mandi Bahauddin 50380, Pakistan*
[***]*Department of Pharmaceutical Sciences, Pak-Austria Fachhochschule Institute of Applied Sciences and Technology, Mang, Khanpur Road, Haripur 22620, Pakistan*
[****]*College of Pharmacy, University of Sargodha, Sargodha 40100, Pakistan*
✉ *Corresponding author: Zulcaif, zulcaif@gmail.com, zulcaif@uorm.edu.pk*

Received March 23, 2026

Transdermal drug delivery of antihistamine offers an alternative to oral administration for the management of atopic conditions. However, the *stratum corneum* is the permeation barrier to drugs, including loratadine, thereby limiting the effectiveness of transdermal systems. The microneedles are the promising approach to overcome this barrier. Microneedles can be prepared with biocompatible and biodegradable polymers. In this research article, microneedle patch was prepared and characterized for drug loading, mechanical strength and dissolution characteristics. *In-vitro* drug penetration on Parafilm M confirmed the microneedle's ability to create uniform microchannels ensuring efficient drug permeation through skin-mimicking layers. The amount of the drug found in the receptor compartment was 87.10 ± 0.62% at 48 hours, whereas that found on the skin was 9.86 ± 0.58%, suggesting a significant amount of drug penetration into the skin. Kinetic modeling of the drug release profile indicated a controlled and sustained drug release pattern. Skin irritation studies confirmed the biocompatibility of the microneedle patches, and showed no signs of edema/irritation up to 48 hours after patch application. These outcomes suggest microneedle patch as an alternative and biocompatible transdermal approach for the safe local delivery of antihistamine.

Keywords: microneedles, transdermal drug delivery, *in-vitro* permeation, antihistamine, microneedle dissolution

INTRODUCTION

In transdermal drug delivery system, microneedle patches have gained researcher interest for drug delivery, offering a minimally invasive and effective alternative for systemic and localized drug administration.[1-3] In contrast to traditional drug delivery methods, microneedle patches generate transient microchannels in the skin, allowing drugs to pass the *stratum corneum*, without inducing significant pain or bleeding.[4-5] Moreover, these systems have gained acceptance in recent years due to their complete dissolution in skin with the absence of residual matrix, least chances of infection and no waste disposal concerns.[6]

Microneedles (MNP) are prepared by using several methods like reactive ion etching, wet chemical etching and solvent casting. However, solvent casting method is most commonly employed for preparation of MNP with natural and synthetic polymers.[7] Hydroxypropyl methylcellulose-E5 (HPMC), a biodegradable, biocompatible and semi-synthetic viscoelastic polymer employed for preparation of MNP.[8] Polyethylene glycol 6000 (PEG 6000) was also employed as MNP matrix former.[9-10]

Generally, the second-generation antihistamine, *i.e.* loratadine, is prescribed in management of allergies like rhinitis, urticarial and other atopic conditions.[11-14] Nevertheless, loratadine is efficacious in clinical practice, has limited water solubility and undergoes extensive first-pass metabolic conversion, leading to a highly variable systemic bioavailability when administered orally.[15-17] Therefore, in order to cope with aforementioned facts and to improve patient compliance, alternative loratadine delivery

approach was required to beat the pharmacokinetic challenges after oral administration. The transdermal delivery of loratadine through microneedle patches avoids hepatic metabolism and thereby improves permeation by delivering the drug in a controlled fashion for an extended time.[9,18-20]

This study aims at formulating and characterizing a loratadine loaded dissolving microneedle patch (MNP) with a polymeric matrix of HPMC E5/PEG 6000 for transdermal drug delivery application. This study is specifically designed to meet the formulation and characterization requirements related to dissolving microneedles by evaluating different aspects such as polymeric composition, mechanical properties, microneedle penetration, drug loading, physicochemical properties, *in-vitro* biodegradation, *ex-vivo* skin permeation, drug release in skin, stability, histological reaction, and skin irritation.[15-17] The specific contribution of this study is the comprehensive evaluation of the formulation of a loratadine loaded dissolving MNP through these characterization techniques, mainly focusing on the mechanical strength of the formulation for skin penetration, while having dissolution and drug loading in the polymeric matrix. The optimization of this formulation for promoting the loratadine skin permeation and local skin reaction were studied further. These results provide evidence for the use of dissolving microneedles for loratadine as a transdermal delivery system; however, the clinical effectiveness of this method was not evaluated in this study.[18-23]

EXPERIMENTAL

Materials

Polyethylene glycol 6000, and hydroxypropyl methylcellulose E5 were purchased from Sigma Aldrich, Germany. Loratadine was gifted by Wilshire Laboratories, Lahore, Pakistan. Silicone molds were purchased from Micropoint Technologies, Singapore. Distilled water was freshly prepared in Research Laboratory of Riphah Institute of Pharmaceutical Sciences at Riphah International University, Lahore Campus.

Methods

Preparation of loratadine-loaded polymeric microneedle patch

To prepare the drug-loaded microneedle patches, the solvent casting method was utilized. HPMC solutions were first prepared at varying concentrations (3-10%) (Table 1) by dissolving the polymer in distilled water.[20] Polyethylene glycol (PEG 6000) was incorporated as a plasticizer at concentrations of 0.2% and 0.5% to enhance the mechanical flexibility of the formulation. Loratadine (20 mg/mL) was dissolved in ethanol and the prepared drug solution was gradually added to the polymeric solution under continuous stirring to ensure the formation of a homogeneous solution. The viscosity and pH of the prepared solutions were measured to ensure formulation uniformity, reproducibility and stability. The drug-loaded polymeric solution was then poured into molds and sonicated for 4 hours. Next, the molds were allowed to dry at room temperature for 48 hours. Patches were carefully peeled off from the molds and stored in airtight containers for further characterization.[24]

Optical evaluation

The optical properties of the prepared microneedle patches were determined using an optical microscope (CX23 Binocular Olympus microscope, Olympus Corporation, Japan). The microneedle patches were placed under the microscope to examine their morphology, uniformity, and needle size. High magnification images of the microneedles were taken to examine their sharpness, size, and distribution in the patches.[25] This step was carried out to affirm if the microneedle patches possess similar morphologies and lack any morphological impairment, such as deformation or breakage, of the microneedles.

Thickness of microneedle patch

The thickness of the MNP was determined using a digital Vernier caliper. The thickness of each sample was determined at three different places to ensure homogeneity across the surface. An average value was obtained for each formula, and this was recorded. This test was important to ensure that there was uniformity in the thickness of each of the patches, which is essential for uniform application and strength.[26]

Mechanical strength

Universal testing equipment Testometric (X350, UK) was employed to check the mechanical strength of MNP. Compression tests were conducted without any fracture or bending. The patch was checked visually by employing a Nikon E200 light microscope, Tokyo, Japan. Morphology was evaluated, serving as a reference for post-compression evaluation like sharpness, breakage and bending. During the compression test, the patch was faced downward on a metal platform by employing the universal testing machine's probe, whose speed was set at 0.5 mm/s by applying a force of 0.02 N for 30 seconds. Subsequently, ascending of the probe was done at the same speed. A light microscope was employed to assess deviations in needle morphology like bending, fracture, breakage and sharpness due to compression.[26]

Tensile strength and percentage elongation

The integrity as well as elongation of selected batches were checked by employing a tensile tester (Pram, China). MNP were kept in between the jaws of the apparatus and pulled mechanically. The difference between initial and final length of the patch was noted. The following formula was employed to check percentage elongation:

$$Elongation\ (\%) = \frac{Lpi}{Lpf} x100 \quad (1)$$

where L_{pi} = initial length, whereas L_{pf} is final length of the patch.

Tensile strength is the optimum stress that a patch can endure, without undergoing breakage until its breaking point is reached. Higher tensile strength results in a rigid patch, which maintains the patch integrity during penetration, thereby reducing the risk of breakage of MNP. Moreover, the elongation percentage depicted the strechability and flexibility of the patch, and was determined by dividing changes in length by original length.[26]

***In-vitro* biodegradation studies**

In-vitro biodegradation studies of the microneedle patches was conducted by employing simulated physiological environment like SBF (simulated body fluid) at 37 °C. After the *in-vitro* biodegradation studies, the patches were evaluated for visual inspection and weight loss.

Moisture content (%)

Moisture analyzer (Sartorius, Germany) was employed to determine the moisture content of all selected MNP in order to evaluate the influence of moisture on their integrity.

Scanning electron microscopy

The surface morphology of the MNP (F8) was analyzed using scanning electron microscopy (SEM). Samples of the microneedles were carefully mounted on aluminum stubs with double-sided adhesive tape and coated with a thin layer of gold to ensure conductivity. The coated samples were then examined under an SEM, and high-resolution images were captured at various magnifications.[27] This analysis aimed to evaluate the microneedle tip sharpness, uniformity, and overall structural integrity.

Fourier transform infrared spectroscopy

Fourier-transform infrared spectroscopy (FTIR) was performed to evaluate the chemical compatibility between the components of the MNP. It includes HPMC-E5, PEG 6000, and Loratadine and Loratadine loaded MNP. The spectra were recorded in the range of 4000-400 cm^{-1} using an FTIR spectrometer (IRTracer-100; Shimadzu).[28]

Differential scanning calorimetry

Differential scanning calorimetry (DSC) was done to record enthalpy changes, phase transition for Loratadine, HPMC, PEG6000 and drug containing MNP (F8) with an increase in temperature. Heating was carried out up to 500 ºC at a rate of a 10 °C rise in temperature per minute. DSC was subjected to calibration in order to obtain validated results.

Thermogravimetric analysis

Thermogravimetric analysis (TGA) depicted weight loss of Loratadine, HPMC, PEG6000 and drug-containing MNP (F8) with a rise in temperature from 0 to 500 °C at a rate of 10 °C per minute.

X-ray diffraction studies

A PW1710 X-ray diffractometer was employed for PXRD studies. The diffractometer was provided with Cu anode and graphite monochromator. The sample was subjected to analysis at 2θ= 0 to 70°.

***In-vitro* penetration study**

The penetration ability of the fabricated MNP was evaluated using Parafilm M as a skin simulant. Parafilm M was folded into seven layers, each approximately 130 µm thick, to simulate the mechanical properties of human skin. The MNP was applied to the surface of the Parafilm M layers (Fig. 5a) and pressed using consistent manual force for 30 seconds to ensure uniform penetration. After the application, the layers were separated, and each was visually examined for microneedle punctures. The penetrated areas on the first through seventh layers were observed under a light microscope to assess the extent and depth of penetration.[29]

Skin irritation study

The irritation potential of the MNP was assessed using albino rats in accordance with ethical guidelines approved by the Animal Ethical Committee of the Animal Ethical Committee of Riphah Institute of Pharmaceutical Sciences, Riphah International University. The dorsal area of each rat was carefully shaved to provide a smooth surface for MNP application (Fig. 6a). A MNP was applied to the shaved area and secured with medical tape to ensure prolonged contact with the skin. The patch was left in place for 24 hours, after which it was removed, and the application site was observed for signs of redness, swelling, or irritation. After 48 hours, the site was reassessed to evaluate any delayed skin reactions (Fig. 6b). Skin reactions were scored based on the Draize irritation scoring system, which evaluates erythema and edema on a scale from 0 to 4.

Drug loading (%)

The drug loading capacity of the MNP was determined to quantify the amount of loratadine incorporated into a single patch. To perform this

analysis, a MNP was dissolved in 10 mL of phosphate buffer solution (pH 7.4) under continuous stirring at 37 °C for 2 hours to ensure complete dissolution of the polymeric matrix and drug. The resulting solution was filtered using a 0.45 µm syringe filter to remove any undissolved particles. The filtrate was analyzed using a UV-visible spectrophotometer at the predetermined λ_{max} of loratadine, *i.e.* 276 nm. The concentration of loratadine in the solution was calculated using a standard calibration curve constructed from different loratadine dilutions in phosphate buffer. The experiment was conducted in triplicate, and the average drug content was calculated to evaluate the drug loading efficiency of the patch.

***Ex-vivo* drug permeation study**

The *ex-vivo* drug permeation study of the prepared loratadine-loaded MNP and pure loratadine solution was conducted using a Franz diffusion cell setup. Rat abdominal skin was taken, washed, and trimmed to remove excess fat, then mounted between the donor and receptor compartments with the *stratum corneum* facing the donor side. The receptor compartment was filled with phosphate buffer solution (pH 7.4) and maintained at 37 °C ± 0.5 °C with continuous stirring. For the *ex-vivo* permeation study MNP, the patch was pressed onto the skin in the donor compartment for sufficient skin penetration, while for the pure loratadine solution, a measured amount of the drug solution was applied. At predetermined intervals, 1 mL of the receptor medium was withdrawn and replaced with fresh medium to maintain sink conditions. The withdrawn samples were analyzed via UV-visible spectrophotometry to determine the cumulative drug release. After 48 hours, the rat skin was crushed, soaked in ethanol, and subjected to sonication to extract any residual drug, which was quantified spectrophotometrically.

The *ex-vivo* drug permeation data for the prepared MNP and pure loratadine solution were analyzed to determine the release kinetics and mechanism of drug permeation. Cumulative drug permeation values were plotted against time and fitted into various kinetic models, including zero-order, first-order, Higuchi, and Korsmeyer-Peppas models. The best-fit model was selected based on the correlation coefficient (R^2) values and the mechanism of drug release. For the Korsmeyer-Peppas model, the release exponent (n) was calculated to interpret the mode of drug release, distinguishing between Fickian diffusion, non-Fickian transport, and case II transport.[30]

Stability studies

Stability studies were performed as per ICH (International Council for Harmonization) guidelines referred as Q1A (R2) for stability testing of new active moieties and drug products. Optimized MNP was subjected to accelerated stability conditions of temperature (40 ± 2 °C) and relative humidity (75 ± 5%) in a stability chamber for up to 9 months. After 0, 1, 3, 6 and 9 months, the optimized batch was subjected to color, shape and thickness of patch, mechanical strength, moisture content and tensile strength testing. The results were assessed by employing ANOVA in order to elucidate changes in the above parameters.[26] The similarity factor (f_2), as well as difference factor (f_1), was employed to check the similarity between F8 before and after stability studies by using DD solver adds in the Microsoft Excel program. The following equations were employed to check the similarity and difference factors:

$$f_1 = \sum_{t=1}^{n} Rt - Tt / \sum_{t=1}^{n} Rt \times 100 \quad (2)$$

$$f_2 = 50 \times \log\{[1+1/n \sum_{t=1}^{n} (Rt - Tt)^2\ ]^{-0.5} \times 100 \quad (3)$$

Histological evaluation

For the histological evaluation, excised skin samples from rats were collected after applying the MNP for a specified duration. The samples were immediately fixed in a 10% formalin solution to preserve tissue integrity. Following fixation, the samples were dehydrated through a graded series of ethanol, cleared with xylene, and embedded in paraffin wax. Thin sections of 5 µm thickness were prepared using a microtome and subsequently stained with hematoxylin and eosin (H&E) staining to observe structural changes under a light microscope. The sections were analyzed for signs of skin disruption, penetration, and inflammation at the application site.

RESULTS AND DISCUSSION

Preparation of loratadine-loaded polymeric MNP

Eight formulations (Table 1) of MNP were prepared via a solvent casting approach and an optimized formulation was further selected. HPMC and PEG-6000 were employed as polymer and permeation enhancer, which imparts fascinating mechanical attributes. Both HMPC and PEG-6000 were used in different ratios and the aim was to tune the ratio of substrate to obtain desired tailored attributes regarding drug release, mechanical strength and needle geometry. The formulation was selected on the basis of optimized structural attributes, as well as for compatibility with the drug, which is mandatory for loratadine loading and release.

FTIR depicted excellent compatibility of polymer (HPMC and PEG-6000) and loratadine, indicating no significant interaction between loratadine and polymer. This ensures compatibility of loratadine with HPMC and PEG within the MNP, the drug retains its therapeutic effectiveness during storage and formulated MNP remains stable up to 9 month. F8 formulation exhibited sharp tips and uniformity of microneedles. Therefore, it was selected for further characterization.

Optical evaluation

The optical analysis of the prepared MNP confirmed their structural integrity and uniformity. As shown in the images (Fig. 1a–c), the microneedles were uniformly distributed across the patch and exhibited sharp tips, as further confirmed by SEM (Fig. 3a), which is essential for effective skin penetration.

Table 1
Composition of microneedle patch (F1 – F8)

Formulation	HPMC, %	PEG, %
F1	3%	0.2%
F2	3%	0.5%
F3	5%	0.2%
F4	5%	0.5%
F5	7%	0.2%
F6	7%	0.5%
F7	10%	0.2%
F8	10%	0.5%

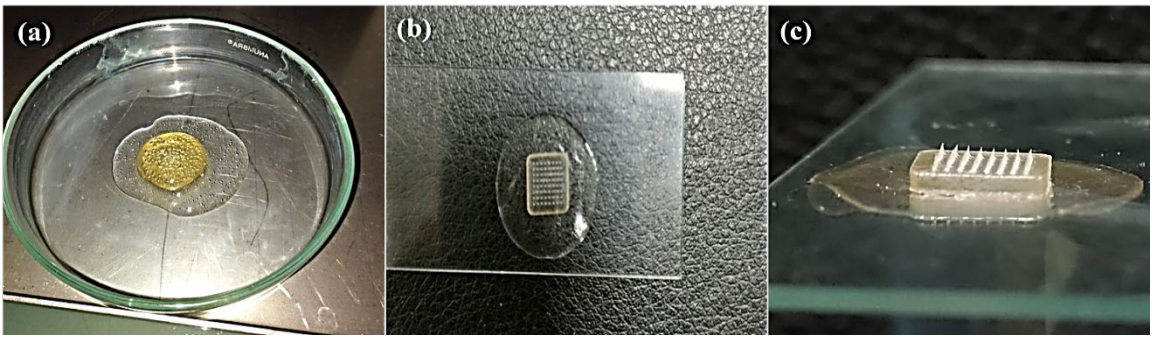


Figure 1: Optical evaluation of microneedle patch, a) polymeric solution poured on silicon mold for drying, b) Arial view of peeled microneedle patch and c) Side view of F8 microneedle patch

Thickness of microneedle patch

The thickness of the microneedle patches was found to be uniform across the surface, with minimal variation. The average thickness was 0.40 ± 0.05 mm. The consistency in thickness across the patches indicates the effectiveness of the fabrication method and the homogeneity of the drug-polymer mixture. Uniform thickness is essential for maintaining the mechanical strength and application efficiency of the MNP, and the results confirm that the prepared patches meet these criteria.

Mechanical strength

Mechanical strength of selected formulations F6, F7 and F8 was 0.8, 0.9 and 1.64 N, respectively. This test was performed to evaluate resistance to deformation under compression and should not be regarded as the direct measurement of the insertion force. The F8 formulation demonstrated the maximum resistance to compression among all tested samples, and thus it was considered the optimum formulation. The penetration potential of the F8 formulation was investigated in the Parafilm M test system separately, where the punctures were visualized through the first four layers and by means of the histological analysis, which proved the creation of the microchannels in the treated area. Both tests confirmed the penetration potential of the optimized patch. Nevertheless, since the original Parafilm M test was performed using a uniform manual force of insertion instead of measuring the force of insertion directly, the present results cannot demonstrate the numerical threshold of 1.64 N of skin-penetration force. As the concentration of PEG-6000 and HPMC increases, mechanical strength increases significantly as both polymers aid in formation of cohesive, dense and thick matrix, thus providing rigidity to nexus. Augmented mechanical strength offers improved skin permeability without undergoing bending and

breakage.[31] Moreover, augmented polymer concentration influences patient comfort. Water soluble polymer (HPMC and PEG) aids in improving dissolution as well as flexibility of microneedles. The optimized concentration of both polymers imparts higher flexibility as well as integrity to the microneedle patch, which is mechanically robust and ensures efficient dissolution upon insertion. Moreover, the optimized formulation containing the tuned blend of PEG and HPMC depicted significant tensile strength (TS). Tailoring polymeric concentration of biodegradable polymer HPMC and PEG, and the type of polymer significantly influence the mechanical strength for transdermal drug delivery for ensuring controlled drug delivery, as reported earlier by Elim *et al*., and Chanabodeechalermrung *et al*.[23,32]

Tensile strength and percentage elongation

Mechanical attributes of MNP were validated by employing mechanical strength and elongation (%) tests. Augmented elongation depicted significant elasticity, which is crucial for skin penetration. The tensile strength of selected formulations F6, F7 and F8 was 8.49 mPa, 9.53 mPa, and 9.97 mPa, respectively. For the same formulations, the elongation percentage was 32.24, 34.54 and 36.34%, respectively, which depicted elasticity and stretchability of the materials. The results were assessed by employing one-way ANOVA of all selected formulations. Significant difference was noted ($p<0.05$) among formulations, affirming that F8 depicted superior mechanical attributes. Post-hoc testing depicted that F8 formulation offered significant tensile strength and percentage elongation, as compared to F6 and F7. The literature survey revealed that a tensile strength of 0.5 mPa prevents breakage of microneedles during skin penetration, which ensures the robustness of microneedles.[26]

***In-vitro* biodegradation studies**

Formulation F8 was subjected to *in-vitro* biodegradation studies up to 7 days, and weight loss (%) was noted as shown in Figure 2. In biodegradation studies, the main mechanism is hydrolysis, which involves penetration of water within the polymeric matrix, leading to breakage of chemical bonds, thereby converting the polymeric matrix into a less complex entity. Moreover, enzymatic degradation also aids in breakdown of the polymeric matrix. PEG degradation results in degradation of ether linkages and resulted in formation of PEG oligomers and ethylene glycol, whereas HPMC degradation includes enzymatic degradation of the cellulose backbone and resulted in formation of hydroxypropyl alcohol and soluble sugars, like xylose and glucose. All these byproducts undergo degradation and are removed from body via excretion.[33]

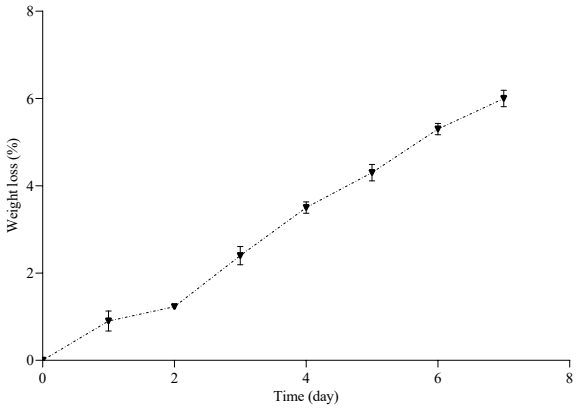


Figure 2: *In-vitro* biodegradation studies of MNP

Moisture content (%)

The moisture content of F6, F7 and F8 was 4.93±0.04%, 4.03±0.89%, and 4.73±0.03%, respectively. The moisture content of all formulations was within the ideal range, thus maintaining the integrity of nexus. Our literature survey revealed that moisture content >5%, weakens the microneedle patch, thereby influencing its skin penetrability, whereas low moisture content (<4%) makes them too brittle, thereby influencing effectiveness.[34-35] Therefore,

moisture content is crucial for maintaining the stability and effectiveness of the patch.

Scanning electron microscopy

Scanning electron microscopy (SEM) analysis of the MNP revealed precise and uniform structural features. As shown in the SEM images (Fig. 3b), the microneedles exhibited sharp, well-defined tips, which are essential for efficient skin penetration. The needles were uniformly distributed across the patch with consistent geometry and dimensions, confirming the effectiveness of the fabrication process. The absence of surface irregularities or deformities further demonstrated the homogeneity and stability of the drug-loaded polymeric solution used during the patch preparation. These findings are consistent with the microscopic analysis (Fig. 3a), which also indicated sharp needle tips and uniform patch structure. The SEM results confirmed that the prepared MNP possess the structural characteristics required for efficient transdermal drug delivery.[26]

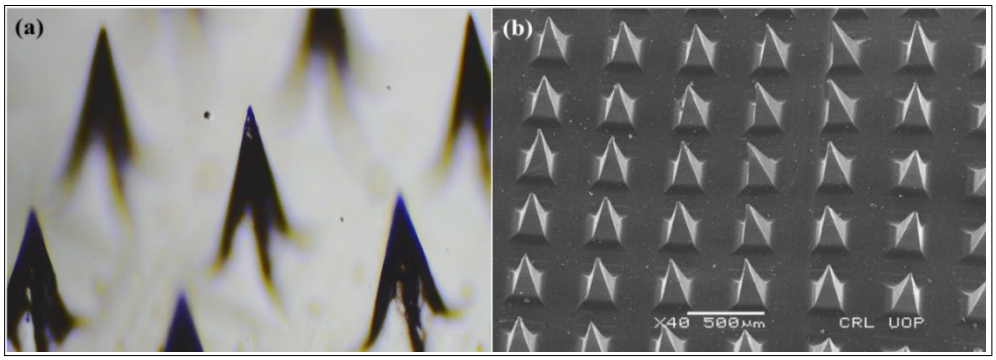


Figure 3: Microscopic evaluation, a) microscopic view and b) SEM image

Fourier transform infrared spectroscopy

Fourier Transform Infrared Spectroscopy (FTIR) was done to evaluate chemical bonds, functional moieties and chemical structure of loratadine, HPMC, PEG-6000 and MNP (F8). FTIR spectra of the individual components and the loratadine-loaded microneedle patch were recorded and shown in Figure 4. The spectrum of HPMC (Fig. 4a) exhibited characteristic peaks corresponding to O–H stretching at approximately 3350 cm^{-1}, C–H stretching at 2920 cm^{-1}, and C–O stretching at 1050 cm^{-1}. Tomar *et al*. formulated HPMC and potassium methyl silonate copolymer and reported similar peaks with minor variation.[36] PEG 6000 (Fig. 4b) displayed prominent peaks for O–H stretching at 3410 cm^{-1} and C–H stretching at 2870 cm^{-1}. Ma and his co-workers formulated HPMC/PMC/CS based thermosensitive polymeric nexus and reported similar peaks.[37] Loratadine (Fig. 4c) demonstrated distinct peaks for aromatic C=C stretching at 1600 cm^{-1} and 1500 cm^{-1}, along with C–N stretching at 1360 cm^{-1}. Similar peaks are previously reported in literature while formulating loratadine-fumeric acid binary complex.[38]

In the FTIR spectrum of the loratadine-loaded microneedle patch (Fig. 4d), the characteristic peaks of loratadine, HPMC, and PEG-6000 were present without significant shifts or changes, indicating the absence of any major chemical interactions or degradation of the drug. However, minor peak intensity changes were observed, which could be attributed to hydrogen bonding between the polymer matrix and loratadine. These findings confirm the compatibility of the components and the stability of loratadine within the microneedle patch formulation.

Differential scanning calorimetry (DSC)

Differential scanning calorimetry (DSC) was conducted to check crystallization, melting point, heat capacity as well as glass transition of loratadine, HPLC, PEG-6000 and MNP. DSC analysis of loratadine depicted well defined pointed endothermic peak at 140 °C, which mimics the melting point of loratadine, which is an indication that loratadine undergoes solid liquid transition (Fig. 5). Moreover, peak sharpness indicates the crystalline nature of loratadine. Makhmalzadeh and his co-workers formulated a loratadine loaded hydrogel and reported similar peaks with minor variation.[39] The DSC thermogram of HPMC depicted a peak at 85-105

°C, which indicates the glass transition temperature (Tg) of HPMC. This sharp endothermic peak also corresponds to dehydration and moisture loss.

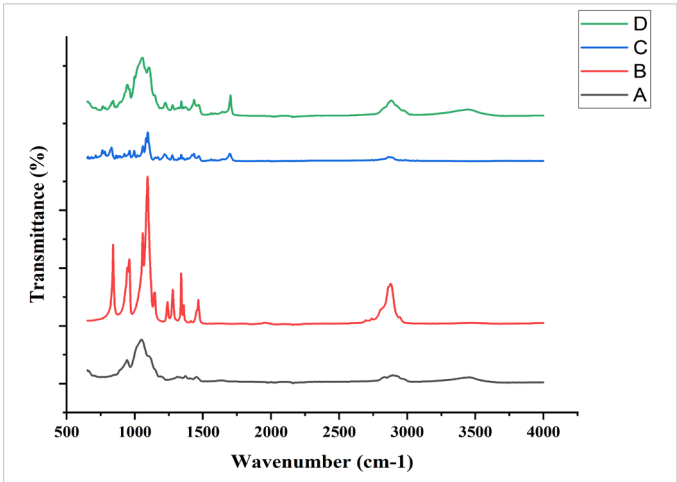


Figure 4: FTIR spectra of a) HPMC, b) PEG-6000, c) loratadine and d) loratadine-loaded microneedle patch

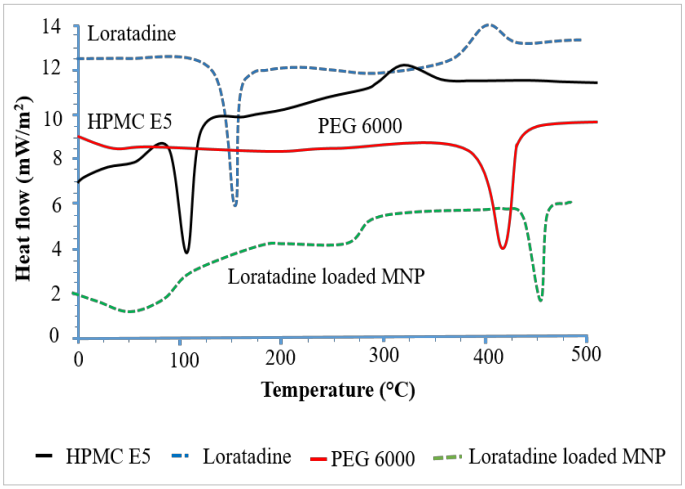


Figure 5: DSC curves of loratadine, HPMC E5, PEG 600 and loratadine-loaded microneedle patch

A few small exothermic peaks at 200-220 °C are indicative of degradation of HPMC, as reported previously by Silva and his co-workers.[40] PEG-6000 showed an endothermic peak at 90 °C, which is also an indication of crystallization temperature. Another peak was observed at 250 °C, which revealed that PEG-6000 retains its stability up to 250 °C. Mandadapu *et al.* reported similar facts.[41]

The loratadine loaded MNP (F8) has a different thermogram, as compared to those of individual components. The DSC thermogram of loratadine revealed a characteristic endothermic melting peak; however, the DSC thermogram of the microneedles loaded with loratadine exhibited a substantial decrease of this thermal phenomenon. This observation is expected because the crystallinity of the drug may have decreased to some extent.

Thermogravimetric analysis (TGA)

Thermogravimetric analysis (TGA) is crucial to assess thermal stability in terms of decomposition behavior of loratadine, HPMC, PEG-6000 and MNP. Thermogravimetric analysis of loratadine depicted primary degradation between 181 °C to 250 °C and corresponds to 40 to 49% weight loss (Fig. 6). The second step of degradation occurs between 250 and 400 °C, and accounts for 35 to 40% degradation. Similar facts were reported previously.[40]

The TGA curve of HPMC depicted two-step degradation. Initially, 40 to 50% degradation occurs from 280 to 320 °C, which is attributed to

cleavage of glycosidic bongs, as well as side chain moieties like OH- and CH_3 moieties. Then, a weight loss of 30 to 35% occurs from 321 to 390 °C, and results in the production of low molecular weight components. Silva and his co-workers reported similar findings.[40]

The thermal behaviour of PEG-6000 depicted 1-3% weight loss, which is attributed to moisture loss. About 70 to 80% degradation was observed at 290 to 400 °C, which is attributed to cleavage of ester linkage. Similar findings were reported by Mandadapu *et al.*[41] The TGA curve of loratadine loaded MNP showed 60% weight loss at 400 °C, thereby indicating the stability of the drug within the microneedle patch.

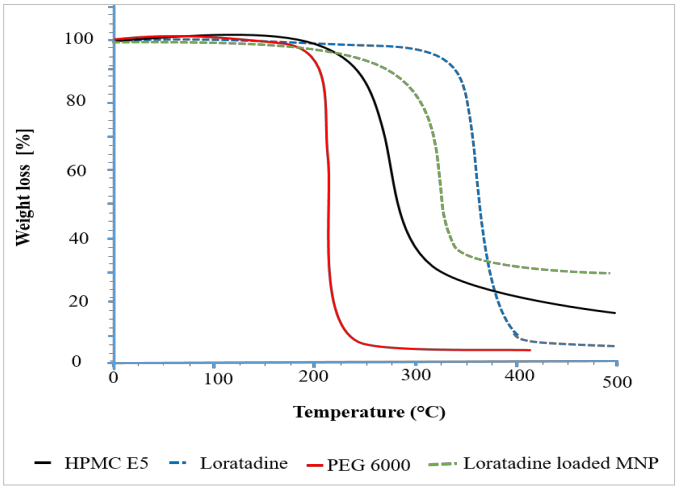


Figure 6: TGA curves of loratadine, HPMC E5, PEG 600 and loratadine-loaded microneedle patch

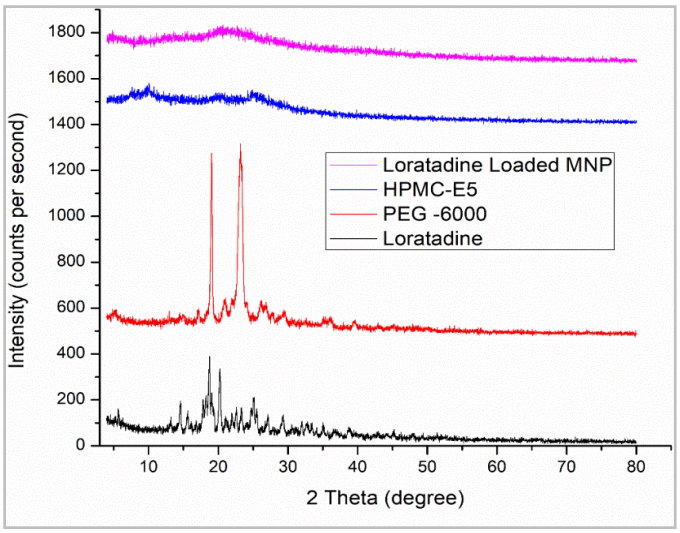


Figure 7: XRD patterns of loratadine, HPMC E5, PEG 600 and loratadine-loaded microneedle patch

X-ray diffraction studies

XRD studies were performed to elucidate the crystalline, semi-crystalline and amorphous nature of loratadine, HPMC, PEG-6000 and MNP. The XRD pattern of loratadine depicted well-defined peaks at 2θ = 22°, 27°, 30°, 38°, 40°, 66° and 69°, which indicates the crystalline nature of loratadine. Alwossabi *et al.* formulated loratadine-based tablets and reported similar peaks with few variations, which also affirms the crystalline nature of loratadine.[42]

The XRD pattern of HPMC E5 depicted a few broad peaks, which indicate its amorphous nature. Zaini *et al.* prepared telmisartan-based solid dispersions with HPMC and reported similar findings.[43] PEG-6000 depicted peaks at 2θ, 15°, 25.37° and 45°, which depict the crystalline nature of PEG-6000; the extent of its crystallization has a

significant influence on drug dissolution and bioavailability. Previous studies also reported similar findings.[44]

The peak intensity of loratadine decreased in the MNP prepared by solvent casting, indicating that the crystalline nature of the drug was converted into an amorphous form after entrapment in MNP, thereby loratadine retained its stability, as shown in Figure 7.

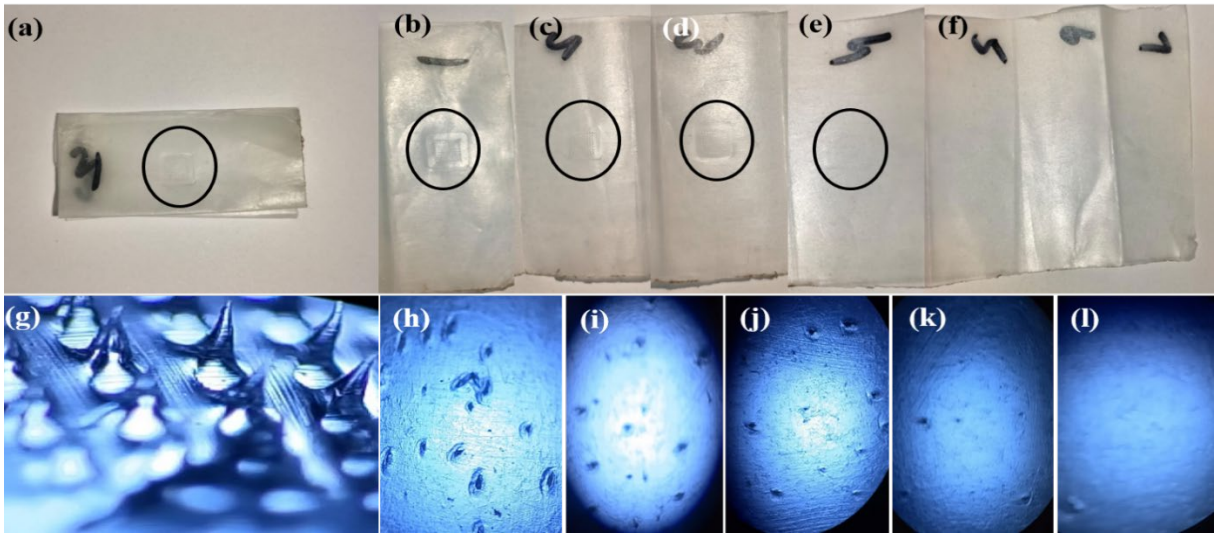


Figure 8: *In-vitro* penetration: a) Patch applied on parafilm M, b) First layer of parafilm M, c) 2nd layer of parafilm M, d) 3rd layer of parafilm M, e) 4th layer of parafilm M, f) 5-7th layers of parafilm M; Microscopic view of g) microneedle patch, h) 1st layer of parafilm M, i) 2nd layer of parafilm M, j) 3rd layer of parafilm M, k) 4th layer of parafilm M, l) 5th layer of parafilm M (showing no penetration)

***In-vitro* penetration study**

The results of the *in-vitro* penetration study demonstrated that the MNP effectively penetrated the upper layers of the Parafilm M model (Fig. 8a). Visible puncture marks were observed on the first four layers (Fig. 8b-8e), indicating the successful penetration of the microneedles. The number and depth of the punctures decreased with increasing depth, with minimal or no penetration observed in the fifth to seventh layers (Fig. 8f). Microscopic analysis (Fig. 8g) confirmed distinct puncture marks on the first (Fig. 8h), second (Fig. 8i), third (Fig. 8j), and fourth (Fig. 8k) layers, while no punctures were visible in the deeper layers (Fig. 8l). These findings highlight the ability of the microneedles to penetrate simulated skin layers effectively, reaching depths sufficient for transdermal drug delivery. Anbazhagan and Suseela formulated insulin coated microneedle patch and depicted that approximately 90% insulin penetrates the skin, skin penetration confirming the robustness of the patch.[45]

Skin irritation study

Rats are frequently employed in order to evaluate tissue response to MNP. The results of the irritation study indicated that the microneedle patch (F8) was well-tolerated by the rats (n=3). Upon removal of the patch after 24 hours, no significant signs of erythema, edema, or other visible irritation were observed at the application site. Similarly, no delayed reactions were noted during the 48-hour observation period. The Draize irritation score for all subjects remained at 0, confirming the safety of the microneedle formulation. These findings demonstrate the safety of the fabricated microneedle patch for transdermal application. The absence of irritation suggests that the materials used in the patch, including HPMC, PEG 6000, and loratadine, are non-irritating, cause no pain or tenderness, edema and pruritus.

Studies have demonstrated that properly formulated MNP caused minimal irritation as compared to tradition transdermal drug delivery systems. Javad *et al.* formulated MNP and reported similar findings.[26]

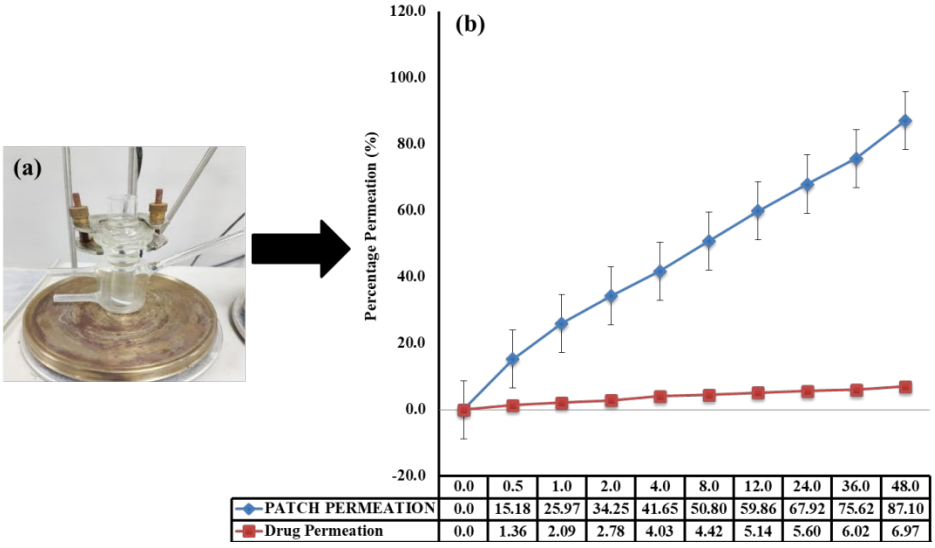
Drug loading efficiency

The drug loading efficiency of the loratadine-loaded microneedle patch (F8) was found to be high, with an average of 98.54% of the drug recovered from a single patch. This high recovery

rate indicates efficient incorporation of loratadine into the microneedle matrix during the formulation process. The uniform distribution of the drug within the polymeric solution, ensured by continuous stirring before pouring into the molds, likely contributed to the minimal drug loss. Furthermore, the compatibility between the polymer (HPMC), plasticizer (PEG-6000), and loratadine, as suggested by the FTIR studies, prevented drug degradation or loss during the preparation and drying stages. The high drug loading also demonstrates the robustness of the preparation method in achieving a reliable and reproducible formulation, making the microneedle patch suitable for effective transdermal delivery of loratadine. Liu *et al*. formulated Astragalus membranous based polysaccharide nanoparticles and reported robustness of drug loading.[46]

Ex-vivo drug permeation study

Ex-vivo permeation studies were carried out by employing rat skin; the studies help understand the interaction of skin and MNP, including diffusion and penetration of patches (n=3). These studies also help to quantify the concentration of loratadine that penetrates skin. The *ex-vivo* permeation study revealed that 87.10% ± 0.62% of the drug from the microneedle patch successfully permeated through the rat skin into the receptor medium over 48 hours. Additionally, 9.86% ± 0.58% of the drug was recovered from the rat skin after extraction, suggesting effective deposition of the drug within the dermal layers. In contrast, only 6.97% ± 0.54% of the drug permeated through the skin from the pure loratadine solution, indicating the superior delivery efficiency of the microneedle patch. The significant enhancement in drug permeation from the microneedle patch can be attributed to the ability of microneedles to bypass the *stratum corneum* barrier, creating microchannels for direct drug entry into the skin layers. The controlled drug release profile observed from the patch aligns with the sustained-release properties imparted by the polymeric matrix. Figure 9 depicts the results of the *ex-vivo* drug permeation study via Franz cell, and permeation comparison between the pure loratadine solution and the prepared microneedle patch.



	0.0	0.5	1.0	2.0	4.0	8.0	12.0	24.0	36.0	48.0
PATCH PERMEATION	0.0	15.18	25.97	34.25	41.65	50.80	59.86	67.92	75.62	87.10
Drug Permeation	0.0	1.36	2.09	2.78	4.03	4.42	5.14	5.60	6.02	6.97

Figure 9: *Ex-vivo* drug permeation study, a) Franz cell and b) Permeation comparison between pure loratadine solution and prepared microneedle patch

Kinetics of *ex-vivo* permeation

The kinetic modeling of the *ex-vivo* drug permeation data revealed distinct differences in the release profiles of the microneedle patch and pure loratadine solution. The *ex-vivo* permeation study for the optimized microneedle design provided the best correlation with the Korsmeyer-Peppas model (R^2 = 0.99). The value of the exponent n was calculated as 0.61. Since these results come from an *ex-vivo* skin permeability study, the value of n is used as an indicator of the general time-dependent permeability process and not as proof of any particular drug release mechanism. This behavior could be the result of several processes taking place together, including dissolution of the drug from the microneedle matrix, skin

partitioning and diffusion of the drug through the skin.

Stability studies

Stability studies were conducted after 0, 1, 3, 6 and 9 months, to ensure the stability of the microneedle patch with the passage of time. Patch thickness, mechanical strength, percentage elongation, tensile strength and moisture content ensures strength, elasticity, hardness and effective drug loading. Moreover, MNP were again subjected to optical evaluation to assess the color and shape of the microneedle patch. There was no visual alteration in the color or the shape of the microneedle patches after 9 months of the stability test. The moisture content was 4.63 ± 0.23% for month 0, 4.85 ± 0.45% for month 1, 4.23 ± 0.48% for month 3, 4.72 ± 0.42% for month 6, and 4.62 ± 0.42% for month 9, respectively. Therefore, the moisture content showed fluctuations throughout the time period, but did not display a continuous increase in moisture content. Thickness, mechanical strength, percentage elongation, and tensile strength did not vary significantly during storage ($p>0.05$). Javed *et al.* formulated empagliflozin loaded microneedle patch for transdermal drug delivery and reported that the formulated microneedle patch remains stable over time.[26]

Table 2
Results of stability studies after 0, 1, 3, 6 and 9 months

Month	Color	Shape	Thickness (mm)	Mechanical strength (N)	% Elongation	Tensile strength (mPa)	Moisture content (%)
0	No change	Intact	0.40 ± 0.05	1.54±0.09	32.34	8.47	4.63±0.23
1	No change	Intact	0.40±0.05	1.56±0.02	34.23	9.45	4.85±0.45.
3	No change	Intact	0.41±0.04	1.61±0.05	33.23	9.34	4.23±0.48.
6	No change	Intact	0.40±0.02	1.59±0.04	35.34	9.21	4.72±0.42
9	No change	Intact	0.40±0.08	1.58±0.06	34.34	9.23	4.62±0.42.

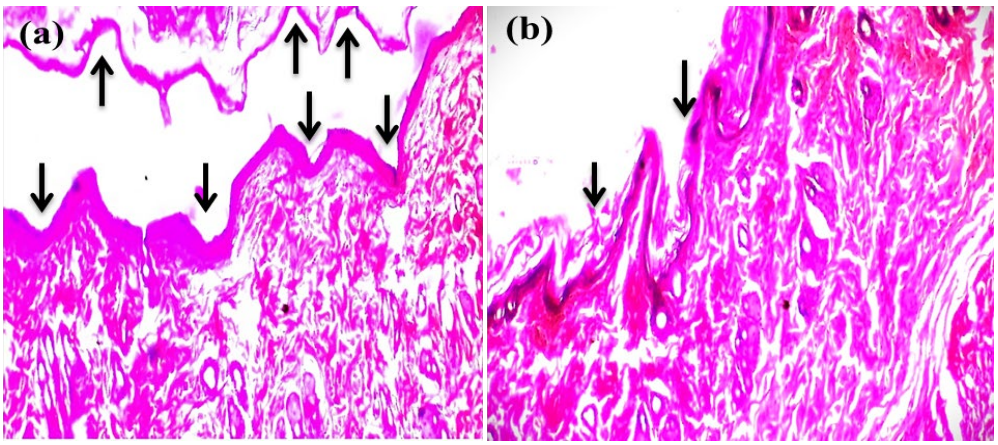


Figure 10: Histology study after microneedle penetration, a) displaying needle penetration, and b) showing deep penetration

Histological evaluation

Histological evaluation of MNP depicted the penetration efficacy and safety of the microneedle patch. Microscopic analysis depicted the creation of microchannels via the microneedle patch, thereby ensuring effective penetration into superficial dermis and through *stratum corneum*. Moreover, due to the microchannels integrity, MNP overcome the primary barrier of *stratum corneum*, thereby enabling skin permeation. The arrows highlight these microchannels, demonstrating the mechanical efficacy of the microneedles in breaching the outermost barrier of the skin, as shown in Figure 10. Additionally, no significant disruption or damage to the deeper dermal layers was observed, indicating that the microneedles were promising for the intended penetration depth.

These findings affirm that the patch design is promising for the delivery of loratadine to the

target tissue, without causing skin damage. Furthermore, the uniformity of distribution and the depth of channels proved reproducibility in the application of the patch. Our results are promising and in line with previous studies, which emphasize the geometry and effectiveness of the material for achieving promising skin penetration.[26]

CONCLUSION

This study successfully prepared and evaluated dissolving MNP for the transdermal delivery of loratadine, offering a novel approach to overcome the limitations associated with oral administration, such as poor water solubility and extensive first-pass metabolism. The MNP demonstrated excellent mechanical properties, effective skin penetration, and controlled drug release, as evidenced by *in-vitro* and *ex-vivo* studies. The overall drug permeability obtained was 87.10 ± 0.62% after 48 hours, while 9.86 ± 0.58% of the drug was found retained on the skin surface. This observation represents local retention of the drug on the skin surface and is mentioned merely descriptively, without any categorization. Histological evaluation confirmed the biocompatibility of the patches, with no significant skin damage or irritation observed after application. These findings suggest that dissolving MNP represent a safe, effective, and patient-friendly alternative for the transdermal delivery of loratadine.

REFERENCES

[1] R. Kaur and V. Arora, in *E3S Web of Conferences*, Italy, July 27-28, 2023, pp. 23, vol. 509, 2024, https://doi.org/10.1051/e3sconf/202450902002

[2] S. Mdanda, P. Ubanako, P. P. D. Kondiah, P. Kumar and Y. E. Choonara, *Polymers*, **13**, 2405 (2021), https://doi.org/10.3390/polym13152405

[3] Q. Zhou, H. Li, Z. Liao, B. Gao and B. He, *Anal. Chem.*, **95**, 515 (2023), https://doi.org/10.1021/acs.analchem.2c01895

[4] V. M. Desai, S. Priya, S. Gorantla and G. Singhvi, *Pharmaceutics*, **15**, 14 (2023), https://doi.org/10.3390/pharmaceutics15010014

[5] N. Sultana, A. Waheed, A. Ali, S. Jahan, M. Aqil *et al.*, *Expert Opin. Drug Deliv.*, **20**, 739 (2023), https://doi.org/10.1080/17425247.2023.2201494

[6] T. Waghule, G. Singhvi, S. K. Dubey, M. M. Pandey, G. Gupta *et al.*, *Biomed. Pharmacother.*, **109**, 1249 (2019), https://doi.org/10.1016/j.biopha.2018.10.078

[7] B. Chanabodeechalermrung, T. Chaiwarit, S. Chaichit, S. Udomsom, P. Baipaywad *et al.*, *Polymers*, **16**, 452 (2024), https://doi.org/10.3390/polym16040452

[8] S. Mudhol and M. S. Peddha, *J. Drug Deliv. Sci. Technol.*, **80**, 104120 (2023), https://doi.org/10.1016/j.jddst.2022.104120

[9] N. N. Aung, T. Ngawhirunpat, T. Rojanarata and P. Patrojanasophon, *AAPS PharmSciTech*, **21**, 25 (2020), https://doi.org/10.1208/s12249-019-1599-1

[10] P. T. Ko, I. C. Lee, M. C. Chen and S. W. Tsai, *J. Taiwan Inst. Chem. Eng.*, **51**, 1 (2015), https://doi.org/10.1016/j.jtice.2015.01.003

[11] L. K. Golightly and L. S. Greos, *Drugs*, **65**, 341 (2012), https://doi.org/10.2165/00003495-200565030-00004

[12] G. W. Canonica and M. Blaiss, *World Allergy Organ. J.*, **4**, 47 (2011), https://doi.org/10.1097/WOX.0b013e3182093e19

[13] A. Nieto, M. Nieto and Á. Mazón, *Expert Opin. Pharmacother.*, **22**, 511 (2020), https://doi.org/10.1080/14656566.2020.1830970

[14] M. N. Fein, D. A. Fischer, A. W. O'Keefe and G. L. Sussman, *Allergy Asthma Clin. Immunol.*, **15**, 61 (2019), https://doi.org/10.1186/s13223-019-0375-9

[15] I. C. Lee, W. M. Lin, J. C. Shu, S. W. Tsai, C. H. Chen *et al.*, *J. Biomed. Mater. Res. A*, **105**, 84 (2017), https://doi.org/10.1002/jbm.a.35869

[16] M. C. Chen, K. Y. Lai, M. H. Ling and C. W. Lin, *Acta Biomater.*, **65**, 66 (2018), https://doi.org/10.1016/j.actbio.2017.11.004

[17] Z. Zhu, L. Huafei, L. Wangding, L. Hansen, W. Yubo *et al.*, *Pharm. Res.*, **31**, 3348 (2014), https://doi.org/10.1007/s11095-014-1424-1

[18] A. Z. Alkilani, M. T. McCrudden and R. F. Donnelly, *Pharmaceutics*, **7**, 438 (2015), https://doi.org/10.3390/pharmaceutics7040438

[19] A. H. Sabri, Y. Kim, M. Marlow, D. J. Scurr, J. Segal *et al.*, *Adv. Drug Deliv. Rev.*, **153**, 195 (2020), https://doi.org/10.1016/j.addr.2019.10.004

[20] R. Parhi, *J. Drug Deliv. Sci. Technol.*, **75**, 103639 (2022), https://doi.org/10.1016/j.jddst.2022.103639

[21] D. Yang, M. Chen, Y. Sun, Y. Jin, C. Lu *et al.*, *Acta Biomater.*, **121**, 119 (2021), https://doi.org/10.1016/j.actbio.2020.12.004

[22] T. Liu, J. Fu, M. Chen, Q. Wu, G. Quan *et al.*, *Eur. Polym. J.*, **210**, 113008 (2024), https://doi.org/10.1016/j.eurpolymj.2024.113008

[23] D. Elim, A. M. N. Fitri, M. A. S. B. Mahfud, N. Afika, N. A. F. Sultan *et al.*, *Colloids Surf. B Biointerfaces*, **222**, 113018 (2023), https://doi.org/10.1016/j.colsurfb.2022.113018

[24] I. C. Lee, J. S. He, M. T. Tsai and K. C. Lin, *J. Mater. Chem. B*, **3**, 276 (2015), https://doi.org/10.1039/C4TB01555J

[25] S. A. Coulman, J. C. Birchall, A. Alex, M. Pearton, B. Hofer *et al.*, *Pharm Res.*, **28**, 66 (2011), https://doi.org/10.1007/s11095-010-0167-x

[26] A. Javed, R. M. Sarfraz, A. Mahmood, Z. Ahmad, M. R. Akram *et al.*, *Naunyn Schmiedebergs Arch. Pharmacol.*, **398**, 6739 (2025), https://doi.org/10.1007/s00210-024-03708-1

[27] C. S. Kolli and A. K. Banga, *Pharm. Res.*, **25**, 104 (2008), https://doi.org/10.1007/s11095-007-9350-0
[28] H. Ijaz, U. R. Tulain, M. U. Minhas, A. Mahmood, R. M. Sarfraz *et al*., *Int. J. Polym. Mater. Polym. Biomater*., **71**, 336 (2022), https://doi.org/10.1080/00914037.2020.1833011
[29] R. X. Liu, Y. T. He, L. Liang, L. F. Hu, Y. Liu *et al*., *J. Ind. Eng. Chem*., **114**, 181 (2022), https://doi.org/10.1016/j.jiec.2022.07.008
[30] G. Roy, R. D. Galigama, V. S. Thorat, P. Garg and V. V. K. Venuganti, *Drug Dev. Ind. Pharm*., **46**, 1114 (2020),https//doi.org/10.1080/03639045.2020.1776317
[31] V. Shah and B. K. Choudhury, *AAPS PharmSciTech*, **18**, 2936 (2017), https://doi.org/10.1208/s12249-017-0774-5
[32] B. Chanabodeechalermrung, T. Chaiwarit, C. Chaiwarit, S. Chaichit, S. Udomsom *et al*., *Polymers*, **16**, 452 (2024), https://doi.org/10.3390/polym16040452
[33] L. A. Alwan and E. Al-Akkam, *Int. J. Drug Deliv. Technol*., **11**, 656 (2021), https://impactfactor.org/PDF/IJDDT/11/IJDDT,Vol11, Issue3,Article2.pdf
[34] Q. L. Wang, J. W. Ren, B. Z. Chen, X. Jin, C. Y. Zhang *et al*., *J. Ind. Eng. Chem*., **59**, 251 (2018), https://doi.org/10.1016/j.jiec.2017.10.030
[35] M. G. McGrath, S. Vucen, A. Vrdoljak, A. Kelly, C. O'Mahony *et al*., *Eur. J. Pharm. Biopharm*., **86**, 200 (2014), https://doi.org/10.1016/j.ejpb.2013.04.023
[36] P. Tomar, R. Kumar, R. Lakhani, A. Srivastava and V. K. Chhibber, *J. Therm. Anal. Calorim*., **147**, 12417 (2022), https://doi.org/10.1007/s10973-022-11447-9
[37] L. Ma, T. Shi, Z. Zhang, X. Liu and H. Wang, *Gels*, **9**, 667 (2023), https://doi.org/10.3390/gels9080667
[38] F. Alatas, M. Aprilliana and D. Gozali, *Asian J. Pharm. Clin. Res*., **10**, 331 (2017), http://dx.doi.org/10.22159/ajpcr.2017.v10i1.15400
[39] B. S. Makhmalzadeh, A. Salimi and A. Niroomand, *Iran. J. Pharm. Res*., **17**, 460 (2018), https://doi.org/10.22037/ijpr.2018.2201
[40] R. C. Silva, M. G. Trevisan and J. S. Garcia, *J. Therm. Anal. Calorim*., **149**, 9333 (2024), https://doi.org/10.1007/s10973-024-13392-1
[41] G. Mandadapu, P. Kolli, K. V. Gopaiah, R. T. Medarametla and G. Rajesh, *World J. Biol. Pharm. Health Sci*., **19**, 95 (2024), https://doi.org/10.30574/wjbphs.2024.19.1.0409
[42] A. M. Alwossabi, E. S. Elamin, E. M. M. Ahmed, E. A. Ismail, A. Ashour *et al*., *Recent Adv. Drug Deliv. Formul.*, **18**, 208 (2024), https://doi.org/10.2174/0126673878288535240530113418
[43] E. Zaini, L. Fitriani, S. Effendy, D. Noviza and A. Halim, *Orient. J. Chem*., **33**, 873 (2017), https://doi.org/10.13005/ojc/330236
[44] S. Biswal, J. Sahoo, P. N. Murthy, R. P. Giradkar and J. G. Avari, *AAPS PharmSciTech*., **9**, 563 (2008), https://doi.org/10.1208/s12249-008-9079-z
[45] G. Anbazhagan and S. B. Suseela, *Mater. Today Commun*., **41**, 110747 (2024), https://doi.org/10.1016/j.mtcomm.2024.110747
[46] X. Liu, C. Guo, W. Yang, W. Wang, N. Diao *et al*., *Carbohyd. Polym*., **345**, 122574 (2024), https://doi.org/10.1016/j.carbpol.2024.122574